Design of Single Unimodular Waveform With Good Correlation Level Via Phase Optimizations

Xiaohan Zhao, Yongzhe Li and Ran Tao
School of Information and Electronics, Beijing Institute of Technology, Beijing 100081, China
Emails: 3120215436@bit.edu.cn, lyz@ieee.org/yongzhe.li@bit.edu.cn, rantao@bit.edu.cn

***Abstract*—In this paper, we focus on the unimodular waveform design with good correlation property, i.e., with low integrated sidelobe level (ISL). In contrast to existing approaches that commonly involve constraints on the moduli of waveform elements, we come up with the idea of designing the waveform via directly optimizing its phase values. Using this idea, the standard ISL-minimization based waveform design is converted as an unconstrained optimization problem with respect to the phase values of waveform elements, which avoids the repetitive procedure of projecting non-unimodular complex values into the best approximations of constant magnitudes. To this end, we first reformulate the ISL metric into a function of the phase values to be obtained for the waveform, and then solve the new unconstrained ISL-minimization-based waveform design using majorization-minimization techniques. The first-order gradient of the reformulated objective function is derived, by which the majorant of the objective is elaborated. Based on this, we finally tackle the design via iterations, at each of which we obtain a closed-form solution with fast implementations. An algorithm is proposed, with whose simpleness and effectiveness are verified by simulations.**

***Index Terms*—Integrated sidelobe level, gradient, majorization-minimization, phase optimization, unimodular waveform design.**

I. Introduction

Waveform design has been a research field of significant interest over several decades [1]–[6], for which the relevant research is continuously updating witnessed by the emergence of new developments in radar [2], sensing [3], communications [7], etc. It has been widely employed in radar signal processing to attain superiorities such as improved resolution [8], better delay-Doppler ambiguities [9], enhanced robustness on parameter estimation [10], [11], etc. Therein lie the high-quality waveform or signaling strategies.

To obtain certain desirable characteristics of waveforms, polyphase-coded waveforms with constant modulus are commonly employed. Such type of waveform is typically designed on the basis of some criteria. For example, it can be obtained in terms of the minimization/maximization on correlation/sidelobe levels, mutual information or entropy [12], signal-to-interference-plus-noise ratio (SINR) [13], Crame-Rao bound [14], AF shaping [9], etc. Among this criteria, the one that relates to the minimization of correlation levels (or sidelobe levels) of waveform are the most commonly used, which typically involves optimizations on the integrated sidelobe level (ISL), weighted ISL (WISL), or peak sidelobe level (PSL) of waveforms [3].

There already exist studies that achieve good correlation properties from the perspective of ISL/WISL minimization. In [6], the author formulated the ISL/WISL minimization-based design in the frequency domain, wherein an alternative function to approximate the objective for the original design was used. Therein lie the developments of algorithms 'CAN' and 'WeCAN', which are generally considered as the benchmark methods. More recently, the framework of majorization-minimization (MM) [15] has been introduced for designing waveforms with good ISL/WISL performance [16], [17]. The relevant algorithm developments include 'MM-Corr', 'MM-WeCorr' [16], 'ISLNew', and 'WISLNew' [17], etc, and the latter two have been reported to show advanced ISL/WISL performance than the former two algorithms [17]. Other recent studies about waveform design with good correlation properties have been conducted using the alternative direction method of multipliers (ADMM) [18], gradient descent in manifold [19], etc., whose relevant works include [19]–[21] (see also the references therein). Generally, the above algorithms only deal with small/medium-scale code lengths of waveforms, and many of them show slow convergence speed of waveform generation which significantly limits their application in practice.

In this paper, we aim at designing the single unimodular waveform that has good correlation property or low ISL values. We propose an idea of designing the waveform via the direct optimization on the phase values of its elements, which differs from existing approaches commonly involving constraints on the magnitude of the waveform. Using this idea, the standard ISL-minimization-based waveform design is transformed as an unconstrained optimization problem with respect to the phase values of waveform. Therefore, the repetitive projection of non-unimodular complex values into approximating constant magnitudes of waveform in existing method can be avoided. Specifically, we first convert the ISL metric into a new objective function with respect to the phase values of waveform elements. Then, we tackle the newly obtained unconstrained ISL-minimization-based optimization problem via majorization-minimization (MM) techniques [15]. The first-order gradient of the new objective function is derived, whose majoriant is therefore elaborated. Based on this, we finally resolve the optimization problem through iterations, wherein we obtain

This work was supported in part by the National Natural Science Foundation of China (NSFC) under Grants 61901041, 62171029, and U21A20456.

a closed-form solution with fast implementations at each. Corresponding algorithm is proposed, whose simpleness and effectiveness are verified by simulations.

Notations: We use bold lowercase, bold uppercase and italic letters to denote column vectors, matrices, and scalars, respectively. Notations $\lambda_{\max}\{\cdot\}$, $(\cdot)^{\mathrm{T}}$, $(\cdot)^{\mathrm{H}}$, $\odot$, ∇, ∇^2, $\min\{\cdot\}$, $\max\{\cdot\}$, $\preceq$, $\mathcal{O}(\cdot)$, $\mathbf{I}_M$,$\mathrm{Re}\{\cdot\}$ and $\mathrm{Im}\{\cdot\}$ denote the largest eigenvalue of a matrix, transpose, conjugate transpose, Hadamard product, gradient, Hessian, minimum value, maximum value, generalized inequality between matrices, order of complexity, the $M \times M$ identity matrix, real part, and imaginary part, respectively. Moreover, operators $\mathfrak{D}\{\cdot\}$, $\mathcal{F}_p\{\cdot\}$, $\mathcal{G}_p\{\cdot\}$, and $\mathcal{T}\{\cdot\}$ denote forming a diagonal matrix whose main diagonal entries are picked up from the input vector, applying the (2P-1)-point fast Fourier transform (FFT), picking up the first P elements to form a new vector, and constructing a Hermitian Toeplitz matrix whose first column coincides with the input vector, repectively. In addition, $\sin(\cdot)$, $\cos(\cdot)$, $e^{j(\cdot)}$, and $|\cdot|$ are element-wise functions of sine, cosine, exponential, and modulus if the input takes a vector form.

II. Signal Model and Problem Formulation

Let us consider the design of a single waveform with unit-modulus elements for a radar or communication system. We assume the waveform has a code length P, whose elements are stored into a vector denoted by $\mathbf{y} \triangleq [y(1), \ldots, y(P)]^{\mathrm{T}}$. Without loss of generality, the mth waveform element $\mathbf{y}$ takes the form given by $y(m) \triangleq e^{j\Phi_m}$, where Φ_m denotes the phase value of the mth element ranging between $-\pi$ and π arbitrarily.

The auto-correlations of the waveform vector $\mathbf{y}$ at all time lags are denoted by $r(p)$, $p = -P+1, \ldots, P-1$, whose definition is given by [3]

$$r(p) \triangleq \sum_{k=p+1}^{P-1} y(k)y^*(k-p) = r^*(-p), \; \forall p \in \{0, \ldots, P-1\}. \tag{1}$$

Based on (1), the ISL of the waveform vector $\mathbf{y}$ that characterizes the accumulated sidelobes can be expressed as

$$\zeta \triangleq \sum_{\substack{p=1-P \\ p\neq 0}}^{P-1} |r(p)|^2. \tag{2}$$

For the single-waveform design that is of interest, a generalized minimization on the ISL can be enforced to synthesize the waveform with good correlation properties. Toward this end, the ISL-minimization-based waveform design can be formulated as

$$\begin{aligned} \min_{\mathbf{y}} \quad & \zeta \\ \text{s.t.} \quad & |\mathbf{y}(p')| = 1, \, p' = 1, \ldots, P \end{aligned} \tag{3}$$

where the constraints guarantee the unit-modulus property for each element.

III. Unimodular Waveform Design via Direct Phase Optimizations

Considering that the elements of any unimodular waveform are complex and have constant magnitudes equal to 1, we therefore only need to manipulate their phase values to seek the lowest ISL for the waveform. Realizing this fact, we generate the idea of reformulating the ISL ζ into a function with resepct to waveform phases $\{\Phi_m\}_{m=1}^{P}$, which therefore leads to the ISL-minimization based waveform design via direct phase optimization to be presented in the following.

Let us introduce a vector composed of all the P phase values, which is denoted as $\mathbf{z} \triangleq [\Phi_1, \Phi_2, \ldots, \Phi_P]^{\mathrm{T}} \in \mathbb{R}^{P\times 1}$. Then, we can express $\mathbf{y}$ as

$$\mathbf{y} = e^{j\mathbf{z}} = \cos(\mathbf{z}) + j\sin(\mathbf{z}) \tag{4}$$

where the functions $\sin(\cdot)$, $\cos(\cdot)$, and $e^{j(\cdot)}$ are calculated element-wisely, and they maintain such operation style in the following. Using (4), transforming the ISL ζ into frequency domain with some manipulations, we have

$$\zeta = \frac{1}{2P}\sum_{p=1}^{2P}\left(\left((e^{j\mathbf{z}})^{\mathrm{H}}\mathbf{a}_p\mathbf{a}_p^{\mathrm{H}}e^{j\mathbf{z}}\right)^2 - 2P((e^{j\mathbf{z}})^{\mathrm{H}}\mathbf{a}_p\mathbf{a}_p^{\mathrm{H}}e^{j\mathbf{z}}) + P^2\right) \tag{5}$$

where $\mathbf{a}_p \triangleq [1, e^{j\omega_p}, \ldots, e^{j(P-1)\omega_p}]^{\mathrm{T}}$ with $\omega_p = \frac{2\pi}{2P}p$, and the equality can be verified to hold by the result of [17] (see (10) therein). Substituting (4) into (3), the constant-modulus constraints can always be guaranteed, which therefore can be discarded. Hence, the optimization problem (3) can be rewritten as

$$\min_{\mathbf{z}} \; \frac{1}{2P}\sum_{p=1}^{2P}\left(\left(\cos(\mathbf{z})+j\sin(\mathbf{z})\right)^{\mathrm{H}}\mathbf{a}_p\mathbf{a}_p^{\mathrm{H}}(\cos(\mathbf{z})+j\sin(\mathbf{z}))\right)^2 \tag{6}$$

which is an unconstrained optimization problem with respect to $\mathbf{z}$. In order to solve (6), we make use of the majorization-minimization technique. Before proceeding with (6), we present the following result about the majorization of a generalized function that has been shown in [17] (see Lemma 1 therein).

Lemma 1. *If a real-valued function $f(\mathbf{x})$ with respect to a real variable $\mathbf{x}$ is second-order differentiable, and there is a matrix $\mathbf{G}$ satisfying the generalized inequality $\nabla^2 f(\boldsymbol{\xi}) \preceq \mathbf{G}$ for all $\mathbf{x}$, then for each point $\mathbf{x}_0$, the following convex quadratic function*

$$g(\mathbf{x}) = f(\mathbf{x}_0) + \nabla f(\mathbf{x}_0)^{\mathrm{T}}(\mathbf{x}-\mathbf{x}_0) + \frac{1}{2}(\mathbf{x}-\mathbf{x}_0)^T\mathbf{G}(\mathbf{x}-\mathbf{x}_0) \tag{7}$$

majorizes $f(\mathbf{x})$ at $\mathbf{x}_0$.

To find a proper majorization function for the objective of (3) (denoted hereafter as $f(\mathbf{z})$) via Lemma 1, the first-order gradient $\nabla f(\mathbf{z})$ of $f(\mathbf{z})$ and the matrix $\mathbf{G}$ that satisfies $\nabla^2 f(\boldsymbol{\xi}) \preceq \mathbf{G}$ have to be both available. For this purpose, we present the following two lemmas.

Lemma 2. *The first-order gradient of $f(\mathbf{z})$ is given by*

$$\nabla f(\mathbf{z}) = \frac{2}{P}\mathrm{Im}\left\{(\mathcal{T}\{\mathbf{A}^{\mathrm{H}}|\mathbf{A}e^{j\mathbf{z}}|^2\}e^{j\mathbf{z}}) \odot e^{-j\mathbf{z}}\right\}. \quad (8)$$

Proof: Expanding the objective function of (3), we have

$$f(\mathbf{z})=\frac{1}{2P}\sum_{p=1}^{2P}\big((\cos(\mathbf{z}))^{\mathrm{T}}\mathbf{a}_p\mathbf{a}_p^{\mathrm{H}}\cos(\mathbf{z})+(\sin(\mathbf{z}))^{\mathrm{T}}\mathbf{a}_p\mathbf{a}_p^{\mathrm{H}}\sin(\mathbf{z}) - j(\sin(\mathbf{z}))^{\mathrm{T}}\mathbf{a}_p\mathbf{a}_p^{\mathrm{H}}\cos(\mathbf{z}) + j(\cos(\mathbf{z}))^{\mathrm{T}}\mathbf{a}_p\mathbf{a}_p^{\mathrm{H}}\sin(\mathbf{z})\big)^2 \quad (9)$$

whose gradient takes the form as follows

$$\begin{aligned}\nabla f(\mathbf{z})=&\frac{1}{P}\sum_{p=1}^{2P}\big(\cos(\mathbf{z})+j\sin(\mathbf{z})\big)^{\mathrm{H}}\mathbf{a}_p\mathbf{a}_p^{\mathrm{H}}\big(\cos(\mathbf{z})+j\sin(\mathbf{z})\big)\\ &\times\big(-2\mathfrak{D}\{\sin(\mathbf{z})\}\mathrm{Re}\{\mathbf{a}_p\mathbf{a}_p^{\mathrm{H}}\}\cos(\mathbf{z}) + 2\mathfrak{D}\{\cos(\mathbf{z})\}\\ &\times\mathrm{Re}\{\mathbf{a}_p\mathbf{a}_p^{\mathrm{H}}\}\sin(\mathbf{z}) + \mathfrak{D}\{\sin(\mathbf{z})\}(j\mathbf{a}_p^*\mathbf{a}_p^{\mathrm{T}})\sin(\mathbf{z})\\ &-\mathfrak{D}\{\cos(\mathbf{z})\}(j\mathbf{a}_p\mathbf{a}_p^{\mathrm{H}})\cos(\mathbf{z}) + \mathfrak{D}\{\cos(\mathbf{z})\}(j\mathbf{a}_p^*\mathbf{a}_p^{\mathrm{T}})\\ &\times\cos(\mathbf{z}) - \mathfrak{D}\{\sin(\mathbf{z})\}(j\mathbf{a}_p\mathbf{a}_p^{\mathrm{H}})\sin(\mathbf{z})\big). \quad (10)\end{aligned}$$

Using the facts that $\mathrm{Im}\{\mathbf{a}_p\mathbf{a}_p^{\mathrm{H}}\}\sin(\mathbf{z}) - \mathrm{Re}\{\mathbf{a}_p\mathbf{a}_p^{\mathrm{H}}\}\cos(\mathbf{z}) = \mathrm{Re}\{\mathbf{a}_p\mathbf{a}_p^{\mathrm{H}}e^{j\mathbf{z}}\}$ and $\mathrm{Re}\{\mathbf{a}_p\mathbf{a}_p^{\mathrm{H}}\}\sin(\mathbf{z}) + \mathrm{Im}\{\mathbf{a}_p\mathbf{a}_p^{\mathrm{H}}\}\cos(\mathbf{z}) = \mathrm{Im}\{\mathbf{a}_p\mathbf{a}_p^{\mathrm{H}}e^{j\mathbf{z}}\}$, after some straightforward derivations, we can further rewrite $\nabla f(\mathbf{z})$ as

$$\begin{aligned}\nabla f(\mathbf{z})&=\frac{2}{P}\mathrm{Im}\Bigg\{\bigg(\sum_{p=1}^{2P}(e^{j\mathbf{z}})^{\mathrm{H}}\mathbf{a}_p\mathbf{a}_p^{\mathrm{H}}e^{j\mathbf{z}}\mathbf{a}_p\mathbf{a}_p^{\mathrm{H}}e^{j\mathbf{z}}\bigg)\odot e^{-j\mathbf{z}}\Bigg\}\\ &=\frac{2}{P}\mathrm{Im}\left\{(\mathcal{T}\{\mathbf{A}^{\mathrm{H}}|\mathbf{A}e^{j\mathbf{z}}|^2\}e^{j\mathbf{z}}) \odot e^{-j\mathbf{z}}\right\} \quad (11)\end{aligned}$$

where $\mathbf{A} \triangleq [\mathbf{a}_1, \mathbf{a}_2, \cdots, \mathbf{a}_{2P}]^{\mathrm{H}}$, and the second equality is obtained via the fact $\sum_{p=1}^{2P}(e^{j\mathbf{z}})^{\mathrm{H}}\mathbf{a}_p\mathbf{a}_p^{\mathrm{H}}e^{j\mathbf{z}}\mathbf{a}_p\mathbf{a}_p^{\mathrm{H}} = \mathcal{T}\{\mathbf{A}^{\mathrm{H}}|\mathbf{A}e^{j\mathbf{z}}|^2\}$. The proof is complete. ■

Lemma 3. *The generalized inequality $\mathbf{G} \succeq \nabla^2 f(\mathbf{z})$ holds if $\mathbf{G}$ is designed as $\mathbf{G} \triangleq \lambda\mathbf{I}_{\mathrm{P}}$ where*

$$\lambda = 8P^2 - \frac{2}{P}\min\big\{\mathrm{Re}\big\{(\mathcal{T}\{\mathbf{A}^{\mathrm{H}}|\mathbf{A}e^{j\mathbf{z}}|^2\}e^{j\mathbf{z}})\odot e^{-j\mathbf{z}}\big\}\big\}. \quad (12)$$

Proof: Using the fact that $j(\mathbf{a}_p^*\mathbf{a}_p^{\mathrm{T}} - \mathbf{a}_p\mathbf{a}_p^{\mathrm{H}}) = \mathrm{Im}\left\{\mathbf{a}_p\mathbf{a}_p^{\mathrm{H}}\right\}$, we can rewrite (10) into the form as follows

$$\begin{aligned}\nabla f(\mathbf{z}) = \frac{2}{P}\sum_{p=1}^{2P}&|\mathbf{a}_p^{\mathrm{H}}e^{j\mathbf{z}}|^2\big(\mathfrak{D}\{\sin(\mathbf{z})\}\big(\mathrm{Im}\{\mathbf{a}_p\mathbf{a}_p^{\mathrm{H}}\}\\ &\times\sin(\mathbf{z}) - \mathrm{Re}\{\mathbf{a}_p\mathbf{a}_p^{\mathrm{H}}\}\cos(\mathbf{z})\big) + \mathfrak{D}\{\cos(\mathbf{z})\}\\ &\times\big(\mathrm{Re}\{\mathbf{a}_p\mathbf{a}_p^{\mathrm{H}}\}\sin(\mathbf{z}) + \mathrm{Im}\{\mathbf{a}_p\mathbf{a}_p^{\mathrm{H}}\}\cos(\mathbf{z})\big)\big). \quad (13)\end{aligned}$$

Applying the definition of gradient to (10), we obtain $\nabla^2 f(\mathbf{z})$ as follows

$$\begin{aligned}\nabla^2 f(\mathbf{x}) = \frac{2}{P}\sum_{p=1}^{2P}&\big(\mathrm{Im}\{(\mathbf{a}_p\mathbf{a}_p^{\mathrm{H}}e^{j\mathbf{z}})\odot e^{-j\mathbf{z}}\}\mathrm{Im}\{(\mathbf{a}_p\mathbf{a}_p^{\mathrm{H}}e^{j\mathbf{z}})\\ &\odot e^{-j\mathbf{z}}\}^{\mathrm{T}} + |\mathbf{a}_p^{\mathrm{H}}e^{j\mathbf{z}}|^2\mathrm{Re}\left\{\mathfrak{D}\{e^{j\mathbf{z}}\}\mathbf{a}_p\mathbf{a}_p^{\mathrm{H}}\mathfrak{D}\{e^{-j\mathbf{z}}\}\right\}\big)\\ &-\mathrm{Re}\left\{\mathfrak{D}\left\{\mathcal{T}\{\mathbf{A}^{\mathrm{H}}|\mathbf{A}e^{j\mathbf{z}}|^2\}e^{j\mathbf{z}}\odot e^{-j\mathbf{z}}\right\}\right\} \quad (14)\end{aligned}$$

where the result of (11) is used for deriving to the simplified form above, and we omit to show the elementary derivations due to the space limitation.

For the majorizations of the first and second summing components of (14), we use the fact that the inequalities $\lambda_{\max}\{\sum_{p=1}^{2P}\mathbf{q}_p\mathbf{q}_p^{\mathrm{H}}\} \leq \sum_{p=1}^{2P}\mathbf{q}_p^{\mathrm{H}}\mathbf{q}_p \leq 2P^3$ hold if we choose $\mathbf{q}_p \triangleq \mathrm{Im}\{(\mathbf{a}_p\mathbf{a}_p^{\mathrm{H}}e^{j\mathbf{z}})\odot e^{-j\mathbf{z}}\}$ and $\mathbf{q}_p \triangleq \mathfrak{D}\left\{e^{-j\mathbf{z}}\right\}\mathbf{a}_p$ accordingly. As for the third summing component of (14) which is diagonal with real elements, we employ the minimum element of it to construct the majorization function. Hence, we obtain the following generalized inequality, i.e.,

$$\nabla^2 f(\mathbf{x}) \preceq \Big(8P^2 - \frac{2}{P}\min\big\{\mathrm{Re}\big\{(\mathcal{T}\{\mathbf{A}^{\mathrm{H}}|\mathbf{A}e^{j\mathbf{z}}|^2\}e^{j\mathbf{z}}) \odot e^{-j\mathbf{z}}\big\}\big\}\Big)\mathbf{I}_{\mathrm{P}} \quad (15)$$

The proof is complete. ■

In terms of Lemmas 1, 2, and 3, the majorization function for the optimization problem (6) can be written as

$$g(\mathbf{z},\mathbf{z}^{(k)}) = \frac{\lambda}{2}\mathbf{z}^{\mathrm{T}}\mathbf{z}+\Big(\frac{2}{P}\mathrm{Im}\big\{(\mathcal{T}\{\mathbf{A}^{\mathrm{H}}|\mathbf{A}e^{j\mathbf{z}^{(k)}}|^2\}e^{j\mathbf{z}^{(k)}}) \odot e^{-j\mathbf{z}^{(k)}}\big\} - \lambda\mathbf{z}^{(k)}\Big)^{\mathrm{T}}\mathbf{z} + \mathrm{const} \quad (16)$$

Ignoring constant terms in (16), we can rewrite the optimization problem (6) as

$$\min_{\mathbf{z}} \frac{\lambda}{2}\mathbf{z}^{\mathrm{T}}\mathbf{z}+\Big(\frac{2}{P}\mathrm{Im}\big\{\big(\mathcal{T}\{\mathbf{A}^{\mathrm{H}}|\mathbf{A}e^{j\mathbf{z}^{(k)}}|^2\}e^{j\mathbf{z}^{(k)}}\big)\odot e^{-j\mathbf{z}^{(k)}}\big\} - \lambda\mathbf{z}^{(k)}\Big)^{\mathrm{T}}\mathbf{z} \quad (17)$$

whose closed-form solution at the $(k+1)$-th iteration is

$$\mathbf{z}^{(k+1)} = \mathbf{z}^{(k)} - \frac{2}{\lambda P}\mathrm{Im}\Big\{(\mathcal{T}\{\mathbf{A}^{\mathrm{H}}|\mathbf{A}e^{j\mathbf{z}^{(k)}}|^2\}e^{j\mathbf{z}^{(k)}})\odot e^{-j\mathbf{z}^{(k)}}\Big\}. \quad (18)$$

To reduce the computational complexity, we apply the FFT to the calculation of (18). Using the fast implementation that $\mathcal{T}\{\mathbf{A}^{\mathrm{H}}|\mathbf{A}e^{j\mathbf{z}^{(k)}}|^2\}e^{j\mathbf{z}^{(k)}} = 2P\mathcal{F}_P^{-1}\{\mathcal{F}_P\{e^{j\mathbf{z}^{(k)}}\} \odot |\mathcal{F}_P\{e^{j\mathbf{z}^{(k)}}\}|^2\}$, we can further rewrite (18) as

$$\mathbf{z}^{(k+1)} = \mathbf{z}^{(k)} - \frac{4}{\lambda}\mathrm{Im}\Big\{\mathcal{G}_P\{\mathcal{F}_P^{-1}\{\mathcal{F}_P\{e^{j\mathbf{z}^{(k)}}\} \odot |\mathcal{F}_P\{e^{j\mathbf{z}^{(k)}}\}|^2\}\} \odot e^{-j\mathbf{z}^{(k)}}\Big\} \quad (19)$$

whose computational complexity is $\mathcal{O}(PlogP)$. The procedures of the waveform design summarized in Algorithm 1.

Algorithm 1 Single unimodular waveform design via direct phase optimizations

Initialization: P, $\mathbf{z}^{(0)} \leftarrow$ random phase values of waveform elements
repeat
  Calculate λ and $\mathbf{z}^{(k+1)}$ via (12) and (19)
  k=k+1
until convergence
Output: $\mathbf{y} = e^{j\mathbf{z}^{(k+1)}}$

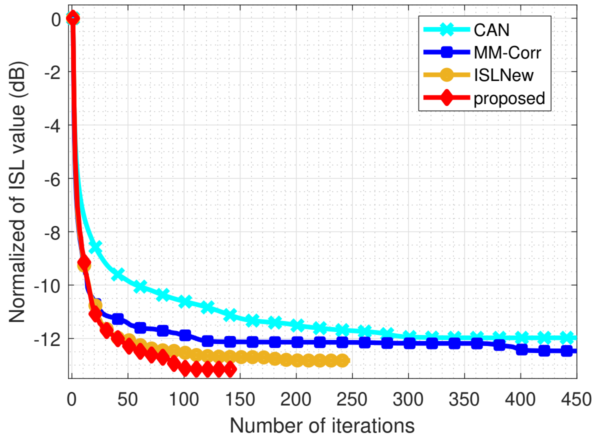

Fig. 1. Normalized ISL versus number of iterations

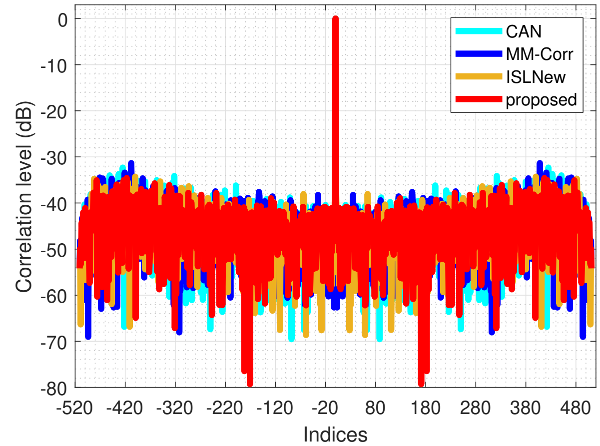

Fig. 2. Correlation level of the tested algorithm

IV. SIMULATION RESULTS

In this section, we evaluate the performance of our proposed algorithm, and compare it with the algorithms 'CAN' of [6], 'MM-Corr' of [16], and 'ISLNew' of [17]. Throughout simulations, we generate random phase values to initialize the unimodular waveform for iterations, and we use the same phase initialization for each comparison. The acceleration scheme SQUAREM [16] is used to speed up the compared algorithms except CAN, and the fast implementation via FFT is applied to algorithms if they allow. The stopping criterion is defined as the absolute ISL difference between two neighboring iterations normalized by the initial ISL, whose tolerance parameter is set to be 10^{-9}.

Example 1: Evaluation on Convergence Speed. We evaluate the convergence speeds of the algorithms tested in terms of ISL values versus the number of iterations. The code length of waveform is chosen as $P = 512$, and the ISL value at each iteration is normalized by the initial ISL. It can be seen from Fig. 1 that our proposed algorithm shows the best convergence speed compared to the other algorithms. The ISLNew algorithm shows the second best convergence speed, while CAN obtains the worst. Moreover, our proposed algorithm achieves the lowest ISL value after convergence with the smallest number of iterations, and the minimum ISL value after convergence is approximately 0.32 dB, 0.52 dB, and 1.01 dB lower than those obtained by ISLNew, MM-Corr, and CAN, respectively.

Example 2: Evaluation on Correlation Property. We evaluate the normalized auto-correlation levels of waveforms generated by the tested algorithms. All parameters are the same as used in the previous example. It can be seen from Fig. 2 that our proposed algorithm gives the best auto-correlation levels of waveform compared to the other three algorithms. The highest correlation level of the waveform generated by our proposed algorithm is around 0.29 dB, 3.23 dB, and 2.25 dB lower than those produced by ISLNew, MM-Corr, and CAN, respectively. optimizes waveform with better auto-correlation property.

Example 3: Evaluation on ISL Versus Code Lengths. We compare the ISL performance in terms of different aspects including the minimum and average ISL values obtained after convergence, the average time consumption, and the average number of iterations. All the results are obtained through 50 independent trials. Two sets of code lengths are tested. One contains medium-scale code lengths given by $\{2^7, 2^8, 2^9, 2^{10}, 2^{11}\}$, and the other contains large-scale code length given by $\{2^{13}, 2^{14}, 2^{15}, 2^{16}, 2^{17}\}$. The corresponding results are shown in Tables I and II, respectively.

It can be seen from Table I that our algorithm outperforms all the other algorithms, which costs around 0.011 seconds and 0.292 seconds for code lengths $P = 2^7$ and 2^{11} (via 123 versus 645 iterations), respectively. For the tested code length $P = 2^{10}$, our proposed algorithm costs around 1.37, 3.18, and 23.67 times less time consumption than those of MM-Corr, ISLNew, and CAN, respectively. It always obtains the lowest average and minimum ISL value compared with all the other algorithms. For all the code lengths larger than $P = 2^7$, our proposed algorithm costs the least number of iterations. The algorithm MM-Corr behaves the second best in terms of the number of iterations for the generation of a single waveform with the medium-scale code lengths.

It can be seen from Table II that the advantage of the proposed algorithm on average time consumption is significant, reducing 53.05, 17.08, and 3.69 times consumption of time compared to MM-Corr, CAN, and ISLNew for the code length $P = 2^{15}$, respectively. Among the tested algorithms, only our proposed algorithm and ISLNew are acceptable for optimizing the waveform of code length $P = 2^{17}$, and they cost 67.963 seconds and 132.441 seconds (via 3262 versus 3680 iterations), respectively. Our proposed algorithm behaves as the fastest algorithm, which also enable the least number of iterations. The ISLNew algorithm behaves as the second best, but it still costs 1.95 to 3.69 times consumption of time more than ours.

V. CONCLUSION

In this paper, we have proposed a fast algorithm to design the single unimodular waveform with good auto-correlation property, wherein the ISL-minimization based design has been

TABLE I
ISL PERFORMANCE OF THE ALGORITHMS TESTED VERSUS MEDIUM-SCALE CODE LENGTH

	$P = 2^7$				$P = 2^8$				$P = 2^9$				$P = 2^{10}$				$P = P = 2^{11}$			
	Min.[a]	Ave.[b]	Iter.[c]	Time[d]	Min.	Ave.	Iter.	Time	Min.	Ave.	Iter.	Time	Min.	Ave.	Iter.	Time	Min.	Ave.	Iter.	Time
CAN	-13.71	-11.69	1450	0.240	-13.05	-12.07	2497	0.543	-13.20	-12.30	2603	0.958	-13.39	-12.54	3269	2.841	-13.03	-12.56	3501	7.257
MM-Corr	-14.37	-12.47	124	0.013	-14.23	-12.89	187	0.036	-13.73	-13.09	292	0.082	-13.99	-13.42	483	0.165	-13.89	-13.50	730	0.416
ISLNew	-15.15	-12.46	125	0.015	-13.99	-12.88	188	0.081	-13.73	-13.10	289	0.164	-13.87	-13.42	456	0.382	-13.75	-13.50	698	0.471
Proposed	-15.15	-12.50	123	0.011	-14.32	-12.90	180	0.027	-13.92	-13.12	277	0.058	-14.00	-13.42	418	0.120	-14.00	-13.51	645	0.292

[a] Min.: Minimum normalized ISL value (in dB). [b] Ave.: Average normalized ISL value (in dB). [c] Iter.: Average number of iteration numbers. [d] Time: Average time consumption (in seconds).

TABLE II
ISL PERFORMANCE OF THE ALGORITHMS TESTED VERSUS LARGE-SCALE CODE LENGTH

	$P = 2^{13}$				$P = 2^{14}$				$P = 2^{15}$				$P = 2^{16}$				$P = P = 2^{17}$			
	Min.[a]	Ave.[b]	Iter.[c]	Time[d]	Min.	Ave.	Iter.	Time	Min.	Ave.	Iter.	Time	Min.	Ave.	Iter.	Time	Min.	Ave.	Iter.	Time
CAN	-13.03	-12.78	7287	29.865	-13.00	-12.85	9547	68.817	-13.02	-12.89	14577	384.704	-	-	-	-	-	-	-	-
MM-Corr	-13.87	-13.66	4891	9.713	-13.85	-13.70	23314	83.844	-13.80	-13.70	118820	1194.476	-	-	-	-	-	-	-	-
ISLNew	-14.07	-13.67	1532	6.158	-13.88	-13.72	2052	15.682	-13.88	-13.75	2724	83.146	-13.87	-13.77	3420	103.249	-13.86	-13.75	3680	132.441
Proposed	-14.04	-13.67	1524	2.330	-13.91	-13.72	2043	5.549	-13.88	-13.74	2663	22.515	-13.85	-13.75	2876	31.102	-13.84	-13.75	3262	67.963

[a] Min.: Minimum normalized ISL value (in dB). [b] Ave.: Average normalized ISL value (in dB). [c] Iter.: Average number of iteration numbers. [d] Time: Average time consumption (in seconds).

solved using the idea of directly optimizing the phase values of waveform elements. In particular, we have reformulated the design problem into an unconstrained optimization problem with respect to the waveform phases, thereby avoiding the repetitive projections of non-unimodular complex values into the best approximations of constant magnitudes. Then, we have elaborated the majorant of the newly obtained objective function based on deriving its first-order gradient, which finally leads to tackling the design via MM techniques with iterations. A closed-form solution with fast implementations has been obtained at each iteration. Simulation results have verified the simpleness and effectiveness of our proposed algorithm for both cases of medium- and large-scale code lengths.

REFERENCES

[1] D. DeLong and E. M. Hofstetter, "On the design of optimum radar waveforms for clutter rejection," *IEEE Trans. Inf. Theory*, vol. 13, no. 3, pp. 454–463, Jul. 1967.

[2] N.Levanon and E.Mozeson, *Radar Signals*. Hoboken, NJ, USA: Wiley, 2004.

[3] H. He, J. Li, and P. Stoica, *Waveform design for active sensing systems: A computational approach*. Cambridge, UK: Cambridge University Press, 2012.

[4] M. C. Wicks, E. L. Mokole, S. D. Blunt, R. S. Schneible, and V. J. Amuso, *Principles of Waveform Diversity and Design*. Raleigh, NC, USA: SciTech Publishing, 2010.

[5] P. Stoica, H. He, and J. Li, "New algorithms for designing unimodular sequences with good correlation properties," *IEEE Trans. Signal Process.*, vol. 57, no. 4, pp. 1415–1425, Apr. 2009.

[6] H. Hao, P. Stoica, and J. Li, "Designing unimodular sequences sets with good correlations—Including an application to MIMO radar," *IEEE Trans. Signal Process.*, vol. 57, no. 11, pp. 4391–4405, Nov. 2009.

[7] D. Tse and P. Viswanath, *Fundamentals of Wireless Communication*. Cambridge University Press, 2005.

[8] K. W. Forsythe and D. W. Bliss, "MIMO radar waveform constraints for GMTI," *IEEE J. Sel. Topics Signal Process.*, vol. 4, no. 1, pp. 21–32, Feb. 2010.

[9] Y. Li, S. A. Vorobyov, and V. Koivunen, "Ambiguity function of the transmit beamspace-based MIMO radar," *IEEE Trans. Signal Process.*, vol. 63, no. 17, pp. 4445–4457, Jun. 2015.

[10] I. Bekkerman and J. Tabrikian, "Target detection and localization using MIMO radar and sonars," *IEEE Trans. Signal Process.*, vol. 54, no. 10, pp. 3873–3883, Oct. 2006.

[11] A. Aubry, A. D. Maio, Y. Huang, and M. Piezzo, "Robust design of radar doppler filters," *IEEE Trans. Signal Process.*, vol. 64, no. 22, pp. 5848–5860, Nov. 2016.

[12] Y. Yang and R. S. Blum, "MIMO radar waveform design based on mutual information and minimum mean-square error estimation," *IEEE Trans. Aerosp. Electron. Syst.*, vol. 43, no. 1, pp. 330–343, Jan. 2007.

[13] J. Li, P. Stoica, and X. Zheng, "Signal synthesis and receiver design for MIMO radar imaging," *IEEE Trans. Signal Process.*, vol. 56, no. 8, pp. 3959–3968, Aug. 2008.

[14] J. Li, L. Xu, P. Stoica, K. W. Forsythe, and D. W. Bliss, "Range compression and waveform optimization for MIMO radar: A Cramér–Rao bound based study," *IEEE Trans. Signal Process.*, vol. 56, no. 1, pp. 218–232, Jan. 2008.

[15] D. R. Hunter and K. Lange, "A tutorial on MM algorithms," *The American Statistician*, vol. 58, no. 1, pp. 30–37, 2004.

[16] J. Song, P. Babu, and D. P. Palomar, "Sequence set design with good correlations properties via Majorization-Mimimization," *IEEE Trans. Signal Process.*, vol. 64, no. 11, pp. 2866–2879, Jun. 2016.

[17] Y. Li and S. A. Vorobyov, "Fast algorithms for designing unimodular waveform(s) with good correlation properties," *IEEE Trans. Signal Process.*, vol. 66, no. 5, pp. 1197–1212, Mar. 2018.

[18] S. Boyd, N. Parikh, E. Chu, B. Peleato, and J. Eckstein, *Distributed Optimization and Statistical Learning via the Alternating Direction Method of Multipliers*. Delft, The Netherlands: now Publisher Inc., Jan. 2011.

[19] A. Khaled, M. Vishal, and R. Muralidhar, "Correlation-gradient-descent: Efficient optimization methods for unimodular waveform design with desirable correlation properties," in *2020 IEEE Int. Radar Conf. (RADAR)*, Apr. 2020, pp. 940–945.

[20] J. Liang, H. C. So, J. Li, and A. Farina, "Unimodular sequence design based on alternating direction method of multipliers," *IEEE Trans. Signal Process.*, vol. 64, no. 20, pp. 5367–5381, 2016.

[21] J. Wang and Y. Wang, "Designing unimodular sequences with optimized auto/cross-correlation properties via consensus-ADMM/PDMM approaches," *IEEE Trans. Signal Process.*, vol. 69, pp. 2987–2999, 2021.